

5 Particle Physics at DESY/HERA (H1)

J. Becker (until April 2005), L. Lindfeld, Katharina Müller, K. Nowak (since November 2005), P. Robmann, S. Schmitt (until May 2005), C. Schmitz, U. Straumann, P. Truöl, and Stefania Xella Hansen

in collaboration with:

N. Berger, M. Del Degan, C. Grab, G. Leibenguth, B. List, M. Sauter, A. Schöning, R. Weber and T. Zimmermann, Institut für Teilchenphysik der ETH, Zürich; S. Egli, R. Eichler, M. Hildebrandt, and R. Horisberger, Paul-Scherrer-Institut, Villigen, and 34 institutes outside Switzerland

(H1 - Collaboration)

5.1 Electron-proton collisions at a centre of mass energy of 320 GeV - summary

Between April 2003 and April 2006 the H1-collaboration has collected 260 pb^{-1} of data from collisions of 27.4 GeV electrons (192 pb^{-1}) and positrons (68 pb^{-1}) with 920 GeV protons with its detector at the HERA storage ring at DESY. Apart from the increased luminosity this post-upgrade HERA-II phase differs from the HERA-I phase (1993-2000) through the availability of both left- and right-handed longitudinally polarized electron and positron beams with polarisations of up to 40%. With this integrated luminosity we have now more than doubled the useful data from the HERA-I phase. That this still falls short of what is needed for searches aiming at beyond the Standard Model physics may be illustrated with the results of a multilepton analysis. Using all available data accumulated between 1994 and 2005 (275 pb^{-1}) multi-lepton (electron or muon) events at high transverse momenta were analysed. The yields of dilepton and trilepton events were found to be in generally good agreement with Standard Model (SM) predictions. Combining all channels, four events are observed with a scalar sum of lepton transverse momenta (ΣP_t) greater than $100 \text{ GeV}/c$, compared to a SM expectation of 1.1 ± 0.2 . These four events are observed in e^+p collisions only where the SM expectation is of 0.6 ± 0.1 and only one of them in the $e\mu$ channel is from the HERA-II data (157 pb^{-1} in this analysis).

However for the vigorous program of both the H1- and the ZEUS-Collaboration dedicated to the exploration of proton structure and tests of quantum chromodynamics (QCD) predictions a wealth of data is available, is being analysed and leads to a continuous flow of publications. This program entails the precise determination of the neutral and charged electroweak current cross sections at high momentum transfer leading to parton density functions in pre-HERA inaccessible domains of Bjorken x and momentum transfer Q^2 , diffractively produced final states, hidden and open charm and beauty production as well as the already mentioned searches for states outside the Standard Model.

5.2 Inner multiwire chamber and vertex trigger

The new five-layer inner multiwire proportional chamber with finer granularity and increased redundancy, equipped with new electronics and a new optical readout delivering signals for an improved z -vertex trigger, which was built by the Zurich group for the upgraded H1-detector, requires only maintenance now. It is an essential ingredient of most H1 trigger combinations, and hence its performance needs to be carefully and continuously moni-

tored by our group members. In November 2005 the opportunity of a HERA maintenance shutdown was used to access the chamber and replace a few broken electronics items, like power supply regulators and optical transmission units.

5.3 Analysis activities

The focus of the Zurich group has now shifted to data analysis. Our contributions deal with excited fermions, where a thesis of a Zürich graduate student has been concluded (1). A τ -lepton analysis has been finished and submitted to a journal (2) (see section 5.3.2 below). Search for lepton flavor violation and photons within jets are studied within the framework of two ongoing Zürich thesis projects. They are nearing conclusion and discussed in Sec. 5.3.3 and 5.3.4 below.

The analysis of HERA-I data in the H1 collaboration lead to 17 publications (2)-(18), of which five are still being reviewed or are in print. Additional, however preliminary results have been communicated to the summer 2005 high-energy physics conferences (19)-(31). These analyses deal in the worst case with about 15 pb^{-1} of data (6; 14) and in the best case with about 120 pb^{-1} of data (2; 10; 11; 18). The first publication from HERA-II running with polarized positrons has appeared in print (32) (27 pb^{-1} righthanded, 21 pb^{-1} lefthanded). An update of the high Q^2 charged and neutral current data taken with polarized electron and proton beams between 2003 and 2006 is given below in Sec. 5.3.1.

A large fraction of these publications deals with searches for states and interactions outside the Standard Model, either of general type (27; 28), or dedicated to specific objects such as excited fermions (1), gravitinos (4), magnetic monopoles (5), leptoquarks (10; 33; 34) and a doubly charged Higgs boson (18). The other two areas, where our group has been active in the past, charm and beauty production (3; 7; 8; 12; 15; 23; 24; 25; 26; 29) benefit strongly from the precise tracking information available from the silicon vertex detector, which was built almost exclusively by the Swiss groups within the H1-collaboration. The studies of the diffractive component of deep inelastic scattering have yielded only to two new results, an analysis of elastic $J\Psi$ - and of high transverse momenta ρ -production (15; 17).

5.3.1 New results from measurements with polarized beams

Data taken with electrons and positrons of different longitudinal polarisation states in collision with unpolarised protons at HERA are used to measure the cross sections of the neutral and charged current processes, $e^\pm p \rightarrow e^\pm X$ and $e^\pm p \rightarrow \nu X$, respectively. The polarisation asymmetry is measured as a function of the four-momentum transfer Q^2 , and compared with the Standard Model prediction. An improved determination of structure function xF_3 is obtained using the new neutral current data in combination with previously published unpolarised data from HERA-I. The HERA-II charged current total cross section analysis so far has been restricted to the kinematical domain $Q^2 > 400 \text{ GeV}^2$ and inelasticity $y < 0.9$. Together with the corresponding cross section obtained from the previously published unpolarised data, the polarisation dependence of the charged current cross section is measured and found to be in agreement with the Standard Model prediction.

Figure 5.1 shows a distribution of the integrated luminosity versus the longitudinal beam polarisation for both directions of the handedness. Considerable variations of the degree of polarisation measured by the polarimeters between 20% and 40% have to be tolerated.

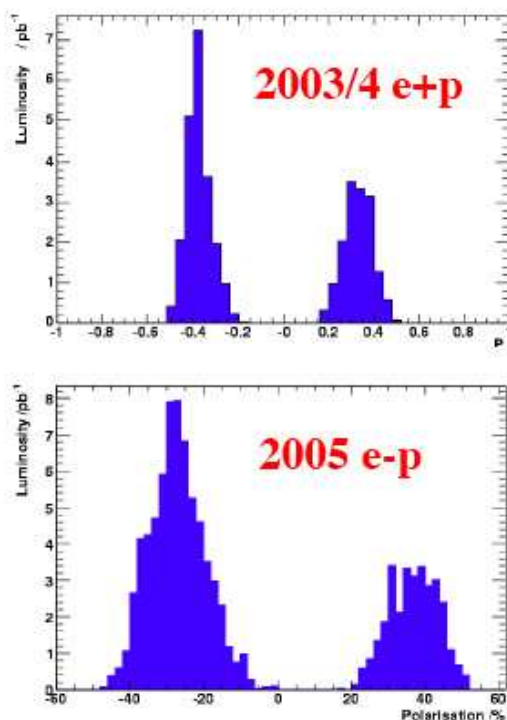


Figure 5.1: Distribution of the integrated luminosity versus polarisation during the two HERA-II running periods with electrons and electrons.

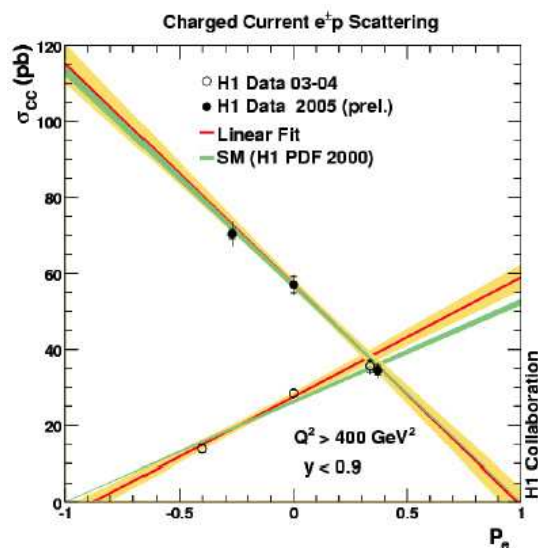


Figure 5.2: Charged current cross section versus polarisation. HERA-II positron (2003/4) and electron data (2005) for $Q^2 > 400 \text{ GeV}^2$ and inelasticity $y < 0.9$ are combined with unpolarised lepton data from 1999/2000 (e^+) and 1998 (e^-). The solid lines represent the standard model predictions using particle density functions derived from H1 neutral current data.

One of the main physics topics with longitudinally polarized leptons at H1 is the direct search for right-handed charged currents using the relation

$$\sigma_{CC} = (1 \pm P) * \sigma_L + (1 \mp P) * \sigma_R .$$

The linear dependence on the polarisation is evident from the data shown in Fig. 5.2. The data shown include those published for e^+p (32), and a 2006 update of the preliminary data shown in summer 2005 (20). The data agree with standard model predictions and do not require right-handed charged currents. A linear fit to the new electron data points given below and displayed in Fig. 5.2 at large momentum transfer ($Q^2 > 400 \text{ GeV}^2/c^2$) and inelasticity $y < 0.9$ yields a result consistent with the SM prediction $\sigma_{CC}(RH) = 0$ at $P_e = 1$:

P	σ_{CC} (pb)	\mathcal{L} (pb^{-1})
-0.272 ± 0.005	70.4 ± 1.2 (stat) ± 3.1 (syst)	70.7
$+0.370 \pm 0.007$	34.5 ± 1.4 (stat) ± 1.5 (syst)	29.7
0	57.0 ± 2.6 (stat) ± 2.4 (syst)	16.4
-1	-0.9 ± 2.9 (stat) ± 1.9 (syst)	

The polarisation uncertainty ($\pm 5\%$) introduces a systematic error of ± 2.9 pb in the result for $P_e = -1$.

For neutral currents the dependence of the cross section on the polarisation is less pronounced, since it enters through the vector (v_e) and axial vector (a_e) quark coupling constants in the electroweak interference between γ and Z -exchange. By measuring both electrons and positrons, polarised and unpolarised one can disentangle the individual quark

flavours:

$$\begin{aligned} \frac{d^2\sigma^{NC}}{dx dQ^2}(e_{L,R}^\pm) &= \frac{2\pi\alpha^2}{xQ^4} \left[(1 + (1-y)^2) F_2^{L,R} + (1 - 1(1-y)^2) xF_3^{L,R} \right] \\ F_2^{L,R} &= \sum_q [xq(x, Q^2) + x\bar{q}(x, Q^2)] \cdot A_q^{L,R} \\ xF_3^{L,R} &= \sum_q [xq(x, Q^2) - x\bar{q}(x, Q^2)] \cdot B_q^{L,R} \\ A_q^{L,R} &= Q_q^2 + 2Q_e Q_q (v_e \pm a_e) v_q \chi_Z + (v_e \pm a_e)^2 (v_q^2 + a_q^2) (\chi_Z)^2 \\ B_q^{L,R} &= \pm 2Q_e Q_q (v_e \pm a_e) a_q \chi_Z \pm (v_e \pm a_e)^2 v_q a_q (\chi_Z)^2 \\ \chi_Z &= \frac{1}{4s_W^2 c_W^2} \frac{Q^2}{Q^2 + M_Z^2} \quad (= 0.67 \text{ at } Q^2 = 10^4 \text{ GeV}^2) \end{aligned}$$

This program however requires high Q^2 and high statistics, as evident from the above expressions and from the data displayed in Figures 5.3 and 5.4. The asymmetry RH/LH increases with Q^2 and reaches values of $\pm 20\%$ for $Q^2 \approx 10^4 \text{ GeV}^2$ for $e^\pm p$ scattering. Only the $e^- p$ data from 2005 are displayed in Fig. 5.3. To enhance the statistical significance of the observed asymmetry one may however combine electron and positron data and plot the ratio

$$R = \frac{\sigma_{NC}(e^+, P_e = +0.336) + \sigma_{NC}(e^-, P_e = -0.270)}{\sigma_{NC}(e^+, P_e = -0.402) + \sigma_{NC}(e^-, P_e = +0.370)}$$

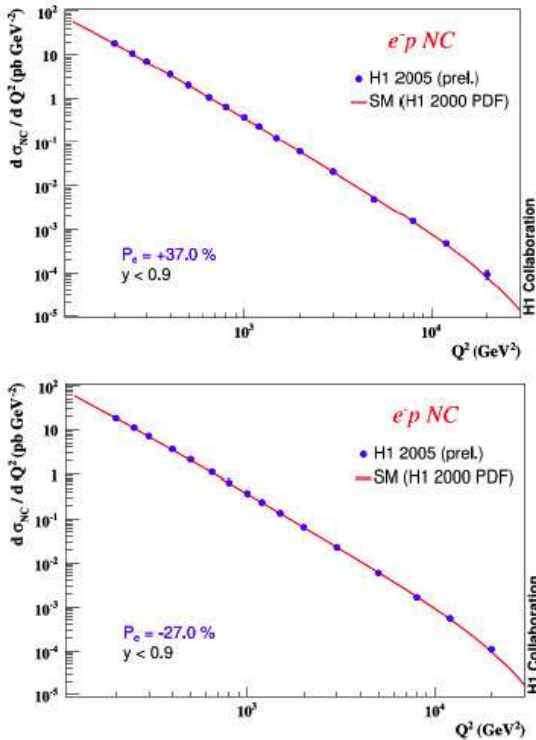


Figure 5.3: Neutral current cross section $d\sigma/dQ^2$ versus momentum transfer for left-handed and righthanded longitudinally polarized electrons.

This is shown in Fig. 5.4. It is apparent that the expectations derived from the particle density functions as extracted from H1 HERA-I data are in good agreement with the data.

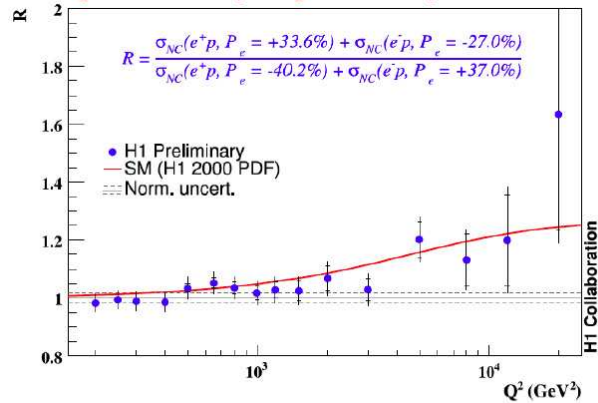


Figure 5.4: Combined neutral current cross section asymmetry from the 2003/2004 positron and the 2005 electron data.

5.3.2 Tau lepton production

Stefania Xella Hansen was involved strongly in an analysis of production of tau lepton pairs ($\tau^+\tau^-$) and a search for events with an isolated tau lepton accompanied by large missing transverse momentum ($\tau + P_t^{\text{miss}}$).

In the Standard Model (SM), tau leptons are produced either in pairs or in association with a tau anti-neutrino, as expected from lepton flavour conservation. In electron/positron-proton collisions, pairs of tau leptons are produced via photon-photon interaction $\gamma\gamma \rightarrow \tau^+\tau^-$ (Fig. 5.5a) (35). Tau leptons and tau anti-neutrinos are produced in W boson decays, as illustrated in Fig. 5.5b (36). The signature of these events is a high transverse momentum (P_t) isolated tau lepton, large missing transverse momentum P_t^{miss} due to the undetected neutrinos, and a hadronic system X , typically of low P_t .

H1 is the first experiment at HERA to perform a measurement of $\tau^+\tau^-$ production. The search for $\tau + P_t^{\text{miss}}$ events complements the previous H1 measurements of the production of events with an isolated electron or muon and large missing transverse momentum, which have revealed an excess over the SM expectation of events containing in addition a high P_t hadronic system (37; 38; 39).

The analysis is based on data from electron/positron-proton collisions at a centre-of-mass energy of 301 or 319 GeV, recorded by the H1 experiment at HERA in the period 1994–2000. The total integrated luminosity amounts to 106 pb^{-1} for the measurement of $\tau^+\tau^-$ production and 115 pb^{-1} for the search for $\tau + P_t^{\text{miss}}$ events.

Two different algorithms to identify hadronic tau decays have been developed for this analysis. The measurement of tau lepton pair production, in which the tau leptons generally have low momentum, requires an optimal background rejection. A Neural Network based identification algorithm is used for this. In contrast, the search for tau leptons produced in W decays at high P_t uses an algorithm that maximises the identification efficiency, since the signal cross section is low and the background is less severe. This algorithm uses the radial size and the charged track multiplicity of the tau jet as discriminators against quark/gluon jets.

The measured cross section for elastic tau pair production $ep \rightarrow ep\tau^+\tau^-$ is $13.6 \pm 5.7 \text{ pb}$. The result is in agreement with the SM expectation of $11.2 \pm 0.3 \text{ pb}$.

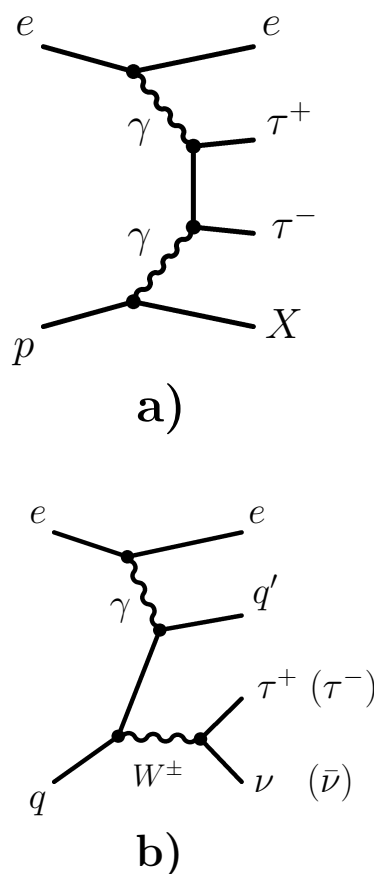


Figure 5.5: Diagrams of the main production mechanisms of tau leptons in electron-proton collisions: a) tau pair production via photon-photon collisions and b) single W boson production followed by the subsequent decay of the W into a tau lepton and a tau anti-neutrino.

In the final event sample of the $\tau + P_t^{\text{miss}}$ search, 6 events are observed in the data, compared to a total SM expectation of $9.9^{+2.5}_{-3.6}$ events, of which $0.89^{+0.15}_{-0.26}$ are expected from SM W production. In the region $P_t^X > 25$ GeV, where an excess of events containing isolated electrons or muons is observed (39), no event is found for a SM prediction of 0.39 ± 0.10 , of which 0.20 ± 0.04 are expected from SM W production.

An upper limit at 95% confidence level is obtained for the production cross section of events containing an isolated tau lepton and large missing transverse momentum in the region $P_t^X > 25$ GeV/c, $\sigma(P_t^X > 25 \text{ GeV/c}) < 0.31$ pb. The present measurement is compatible with the previous measurement of events with an electron or muon and P_t^{miss} , as expected if lepton universality is assumed.

The analysis has been completed and the paper was submitted for publication recently (2).

5.3.3 Search for lepton flavor violation

This analysis is the thesis project of Linus Lindfeld.

In ep collisions, a lepton flavor violating process (LFV) can induce the appearance of a muon or tau instead of the electron in the final state. A convenient concept to explain such exotic signatures is the exchange of a leptoquark. Leptoquarks appear naturally as color triplet scalar and vector bosons in many extensions of the standard model such as Grand Unified Theories (40), Supersymmetry (41), Compositeness (42) and Technicolor (43) allowing for LFV transitions like $e \rightarrow \mu$ and $e \rightarrow \tau$.

After presenting the preliminary H1 result of the search for LFV processes in e^+p -collisions at the summer conferences ICHEP'04 (Beijing) and TAU'04 (Nara), the analysis was extended in 2005 to cover also e^-p -collisions. Analysing additional 13.5 pb^{-1} of e^-p -data taken in 1998-1999 gives sensitivity to $F = 2$ leptoquarks, where the fermion number $F = |3B + L|$ is a combination of the baryon and lepton number of the initial particles. As in the previously analysed e^+p -data, no deviation from the Standard Model is found in the e^-p -data.

Extending the Buchmüller-Rückl-Wyler (BRW) effective model (44) to LFV processes, limits on the Yukawa coupling of all 14 leptoquark types to a muon or tau and a light quark are established. The statistical analysis is completely revised and performed in analogy to the latest

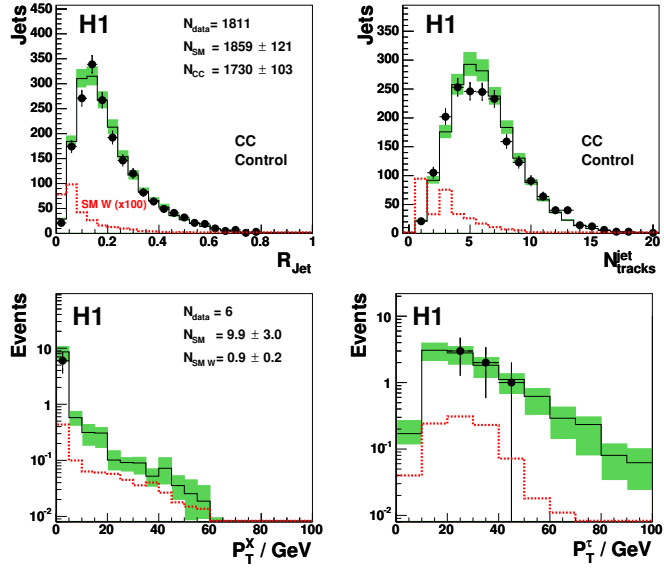


Figure 5.6:

Top: The radius of isolated jets R_{jet} and the number of charged particles $N_{\text{tracks}}^{\text{jet}}$ in isolated jets in the main background (CC) to the $\tau + P_t^{\text{miss}}$ search, at preselection level.

Bottom: The hadronic transverse momentum P_t^X and the transverse momentum P_t^τ of the τ candidate in the final selection of $\tau + P_t^{\text{miss}}$ events. In each figure the data (points) are compared to the SM expectation (solid histogram) shown with its uncertainty (shaded band). The signal contribution dominated by the SM W production is also shown (dashed histogram).

published H1 results of a search for leptoquark bosons (45). This statistical analysis follows a modified frequentist approach and combines different search channels including all systematic uncertainties with correlations. Within this new method, the search for LFV decays of leptoquarks into tau-quark pairs could be extended to processes with a subsequent muonic and electronic decay of the tau lepton. The analysis in the electronic tau decay channel follows a NC DIS selection with additional missing transverse momentum in the electron direction. The search in the muonic tau decay channel is performed in analogy to the search for LFV decays of leptoquarks into muon-quark pairs. The addition of the leptonic channels to the hadronic tau decays improve the tau selection efficiency significantly. Fig. 5.7 shows limits on the Yukawa coupling of scalar (left column) and vector (right column) F=2 leptoquarks to muon-quark pairs (top row) and F=0 leptoquarks tau-quark pairs (bottom row) as a representative example for the interpretation of the analysis. Furthermore, the extended BRW model is opened to arbitrary values of the lepton flavour violating branching ratio β_{LFV} with

$$\beta_{LFV} = \frac{\lambda_{lq}^2}{\lambda_{lq}^2 + \lambda_{eq}^2}, \quad l = \mu, \tau. \quad (5.11)$$

In order to set most stringent limits in the λ_{eq} - λ_{lq} -plane, the published results from the search for first generation leptoquarks (45) are combined with the results of this analysis. The combined limits from the search for tau-quark pairs are illustrated in Fig.5.8. The not shown limits on leptoquarks decaying to muon-quark pairs are slightly more stringent and with similar features.

It is planned to publish these results in summer 2006.

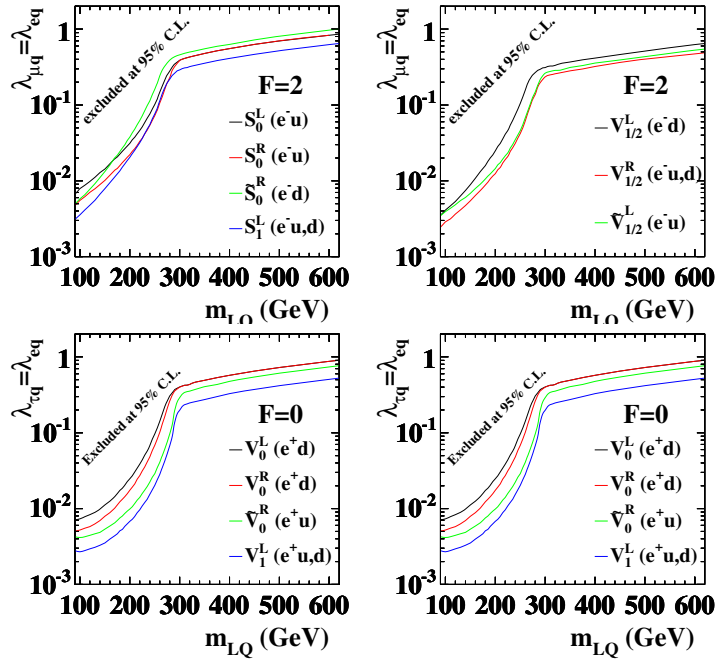


Figure 5.7: Limits on the coupling constant strength $\lambda_{lq} = \lambda_{eq}$ at 95% C.L. as a function of the leptoquark mass for scalar and vector F=2 leptoquarks decaying to a muon-quark pair (top row) and F=0 leptoquarks decaying to a tau-quark pair (bottom row).

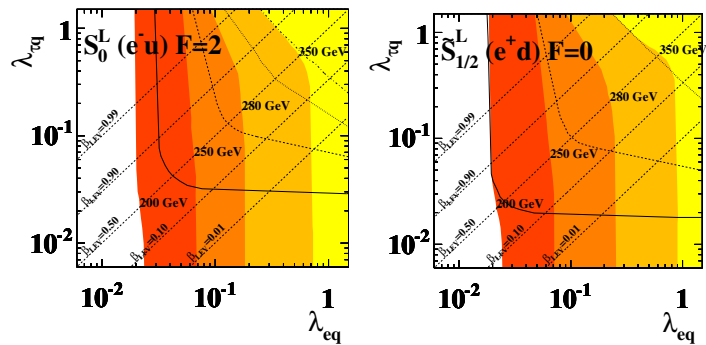


Figure 5.8: Four different masses limits at 95% C.L. on $\lambda_{\tau q}$ as a function of λ_{eq} in a model where the LFV branching ratio $BR = \lambda_{\tau q}^2 / (\lambda_{\tau q}^2 + \lambda_{eq}^2)$ is not fixed (Left: F=2, Right: F=0).

5.3.4 Inclusive prompt photon production

This analysis is the thesis project of Carsten Schmitz. A very close and fruitful cooperation with the members of the theory group at our University, T. Gehrmann, A. Gehrmann-De Ridder and E. Poulsen made it possible to provide in parallel both a novel data analysis and a new theoretical calculation, based on carefully coordinated selection criterias.

Isolated photons with high transverse momentum in the final state are a direct probe of the dynamics of the hard subprocess, since they are directly observable without large corrections due to hadronisation and fragmentation. Previously ZEUS and H1 have measured the prompt photon cross section in photoproduction(46; 47). ZEUS has recently published an analysis of the prompt photon cross section for photon virtualities Q^2 larger than 35 GeV^2 (48). The results are compared to the new leading order calculation of our theory colleagues (49; 50), $\mathcal{O}(\alpha^3)$, that offers first predictions for the inclusive prompt photon production in Deep Inelastic Scattering.

The events have been collected in the years 99/00 at a center of mass energy of 318 GeV , with a total integrated luminosity of 70.6 pb^{-1} . Events were selected with the electron reconstructed in the backward calorimeter (SpaCal(52)). Photons are identified in the liquid argon calorimeter (LAR)(53) by a compact electromagnetic cluster with no track pointing to it. The transverse energy is restricted to $3 \text{ GeV} < E_t^\gamma < 10 \text{ GeV}$ in the pseudorapidity region $-1.2 < \eta_\gamma < 1.8$.

The main experimental difficulty is the separation of the photons from neutral mesons, mainly π^0 or η , since at high energies their decay photons are not resolved but reconstructed in one single electromagnetic cluster. These mesons are mainly produced in hadronic jets, therefore an isolation criterium is applied for the γ candidates. To ease the comparison with pQCD calculations we use an infrared-safe definition of the isolation requirement(54; 55): the energy fraction z of the photon energy to the energy of the jet which contains the photon (Photonjet) has to be larger than 0.9: $z = E^\gamma / E^{\text{Photonjet}} > 0.9$ After the selection cuts there is still a large fraction of background from neutral meson decays. Then the photon signal is extracted by a shower shape analysis which uses six discriminating shower shape functions in a likelihood analysis.

The data are corrected for detector effects by taking the average of the corrections of the PYTHIA 6.2(56) and the HERWIG 6.5(57) event generator. The background from neutral mesons was generated with the RAPGAP(58) generator. However, the background Monte Carlo was only used to control the sample, not for the extraction of the signal. This was done using single particles only.

In a first step events are selected with a good electron and a jet which contains a photon candidate as defined above. In a second step the prompt photon signal is extracted by a likelihood analysis of the shower shapes. The photon candidate clusters are analysed using six different shower shape variables to discriminate between the signal of a single photon and neutral mesons.

- Hot core fraction: fraction of energy deposited in four or eight - depending on the granularity of the calorimeter - contiguous cells including the cell with highest energy.
- Transverse radius of the cluster (transverse plane is perpendicular to the direction of the incoming particle).
- Energy fraction of the hottest cell.

- Energy fraction in the first layer.
- Kurtosis of the transverse energy distribution of the cluster cells.
- Transverse symmetry of the cluster: a photon is expected to have a symmetric cluster ($S=1$), whereas neutral mesons with more than one decay photon are of more asymmetric shape.

Figure 5.9 shows the six different shower shape variables together with the background from RAPGAP as well as photons radiated off the electron as predicted by RAPGAP and the signal prediction from PYTHIA (scaled by 2.3) for photons being radiated off the quark. Both contributions from RAPGAP are used unscaled. All variables are nicely described by the sum of the Monte Carlo predictions.

The estimators are combined in a likelihood analysis as well as a neural net and a range search analysis as a cross check. Monte Carlo studies showed that neutral mesons can be well separated from photons for transverse energies below 10 GeV. Only particles which decay very asymmetrically are misidentified as photons.

The probability densities that are used for the likelihood method are taken from the simulation of single particles. Only the contributing fraction of any neutral meson (π^0 , η^0 , η' , K^0 , ρ , ω , K^* , K_L , K_s , n and \bar{n}) is taken from Monte Carlo simulation (RAPGAP). The likelihood functions are calculated separately for different bins in E_t and different wheels of the calorimeter(53) which correspond to different η_γ ranges. The contribution of photons and neutral mesons is then determined by independent fits to the data using likelihood distributions obtained from a set of single particle photons and background, respectively. The advantage of the use of single particles is that they can easily be produced in high statistics.

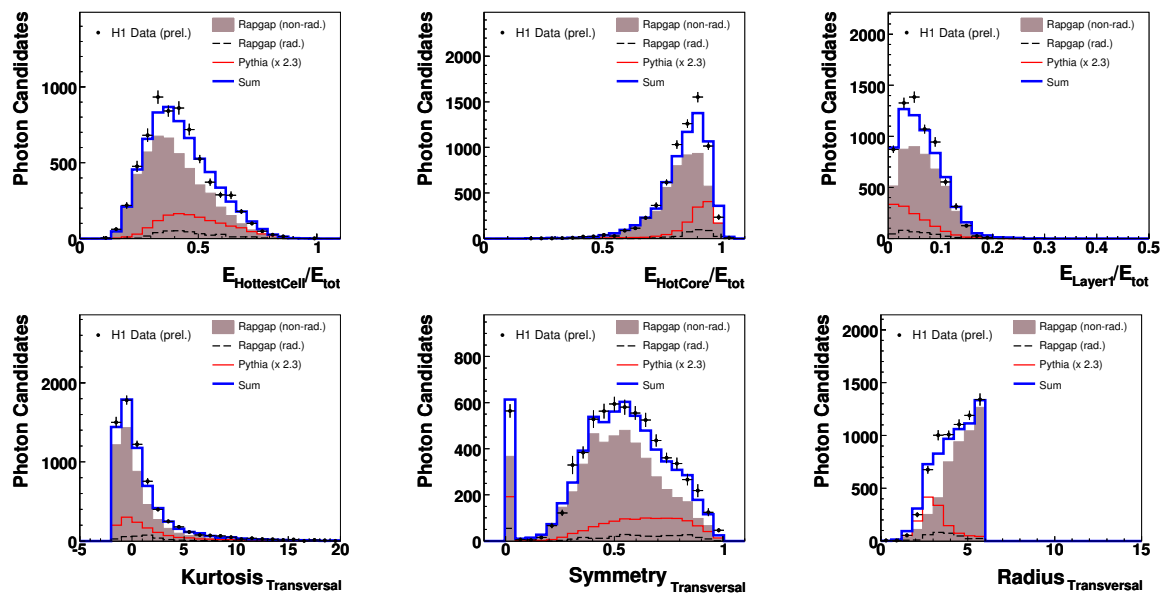


Figure 5.9: Shower shape variables used as input for the discrimination between the photon and neutral mesons: Transverse kurtosis, symmetry and radius and energy fractions of the hottest cell, the hot core and the first layer. The measured data points are shown together with the signal Monte Carlo from PYTHIA, scaled by a factor 2.3, photons radiated off the incoming or outgoing electron (rad) and background from neutral mesons (non-rad) as estimated by RAPGAP. The contributions from RAPGAP are used unscaled. The sum of the Monte Carlo prediction is indicated by the blue line.

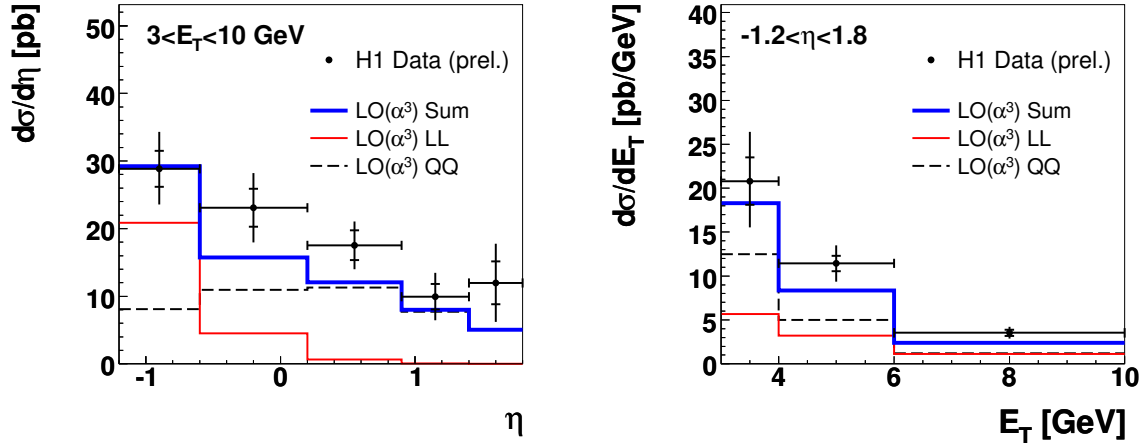


Figure 5.10: Prompt photon differential cross sections $d\sigma/dE_T^\gamma$ for $-1.2 < \eta^\gamma < 1.8$ (a) and $d\sigma/d\eta^\gamma$ (b) for $3 < E_T^\gamma < 10$ GeV, for photon virtualities $Q^2 > 4$ GeV² and $y_e > 0.05$ compared to the LO calculation[49; 50]. LL and QQ show the contribution of radiation off the electron and the quark line, respectively. As the interference of these two contributions is very small it is not shown, but included in the sum.

Differential cross sections for the production of isolated photons in deep inelastic scattering are shown for $Q_e^2 > 4$ GeV², $y_e > 0.05$ for photons with $3 < E_T^\gamma < 10$ GeV, pseudorapidity $-1.2 < \eta^\gamma < 1.8$ and the isolation $z = E_\gamma/E_{\gamma,Jet} > 0.9$. The errors in the figures contain the statistical error and the systematic errors added in quadrature. Figure 5.10 shows the cross section as a function of transverse energy and the pseudorapidity compared to the new LO (α^3) calculation(49; 50) which gives a good description of the data. At large pseudorapidities the dominant contribution comes from radiation off the quark line (QQ), whereas in the backward region the radiation off the electron line (LL) dominates the cross section. The calculation gives a nice description of the data both in shape and in scale in contrast to the Monte Carlo predictions from PYTHIA and HERWIG which are low by a factor 2.3 and 2.6 to describe the data.

The analysis was carried out in close collaboration with the theory group at the University of Zürich. All cuts were carefully adjusted both in the analysis and the LO calculation. It is planned to extend this fruitful collaboration to further measurements with photons in the H1 detector (thesis project of K. Nowak).

- [1] **Search for Excited Quarks at HERA**, Jan Becker, PhD Thesis, University of Zürich (2005)
- [2] **τ -Lepton Production in ep -Collisions at HERA**, H1-Collaboration**, A. Aktas et al., DESY 06 – 029, hep-ex/0604022, submitted to Eur.Phys.J.**C** (2006).
- [3] **Measurement of $F_2^{c\bar{c}}$ and $F_2^{b\bar{b}}$ at High Q^2 using the H1 Vertex Detector at HERA**, H1-Collaboration, A. Aktas et al., DESY 04 – 209, hep-ex/0411046, Eur.Phys.J.**C40** (2005), 349 - 359.
- [4] **Search for Light Gravitinos in Events with Photons and Missing Transverse Momentum at HERA**, H1-Collaboration, A. Aktas et al., DESY 04 – 227, hep-ex/0501030, Phys.Lett.**B616** (2005), 31 - 42.
- [5] **A Direct Search for Magnetic Monopoles Produced in Positron-Proton Collisions at HERA**, H1-Collaboration, A. Aktas et al., DESY 04 – 240, hep-ex/0501039, Eur.Phys.J.**C41** (2005), 133 - 141.
- [6] **Measurement of Dijet Cross Sections for Events with a Leading Neutron in ep Interactions at HERA**, H1-Collaboration, A. Aktas et al., DESY 04 – 247, hep-ex/0501074, Eur.Phys.J.**C41** (2005), 273 - 286.

- [7] **Measurement of Beauty Production at HERA Using Events with Muons and Jets**,
H1-Collaboration, A. Aktas *et al.*, DESY 05 – 004, hep-ex/0502010, Eur.Phys.J. **C41** (2005), 453 - 467.
- [8] **Measurement of Charm and Beauty Photoproduction at HERA $D^*\mu$ Correlations**,
H1-Collaboration, A. Aktas *et al.*, DESY 05 – 040, hep-ex/05003038, Phys.Lett. **B621** (2005), 56 - 71.
- [9] **Measurement of Deeply Virtual Compton Scattering at HERA**,
H1-Collaboration, A. Aktas *et al.*, DESY 05 – 065, hep-ex/0505061, Eur.Phys.J. **C45** (2005), 1 - 11.
- [10] **Search for Leptoquark Bosons in ep Collisions at HERA**,
H1-Collaboration**, A. Aktas *et al.*, DESY 05 – 087, hep-ex/0506044, Phys.Lett. **B629** (2005), 9 - 19.
- [11] **A Determination of Electroweak Parameters at HERA**,
H1-Collaboration**, A. Aktas *et al.*, DESY 05 – 093, hep-ex/0507080, Phys.Lett. **B632** (2006), 35 - 42.
- [12] **Measurement of F_2^{cc} and F_2^{bb} at Low Q^2 Using the H1-vertex Detector at HERA**,
H1-Collaboration**, A. Aktas *et al.*, DESY 05 – 110, hep-ex/0507081, Eur.Phys.J. **C45** (2006), 23 - 33.
- [13] **Measurement of Event Shape Variables in Deep Inelastic Scattering at HERA**,
H1-Collaboration**, A. Aktas *et al.*, DESY 05 – 225, hep-ex/0512014, Eur.Phys.J. **C46** (2006), 343 - 356.
- [14] **Forward Jet Production in Deep Inelastic Scattering at HERA**,
H1-Collaboration**, A. Aktas *et al.*, DESY 05 – 135, hep-ex/0508055, Eur.Phys.J. **C46** (2006), 27 - 42.
- [15] **Elastic J/ψ Production at HERA**,
H1-Collaboration**, A. Aktas *et al.*, DESY 05 – 161, hep-ex/0510016, Eur.Phys.J. **C** (2006), in print.
- [16] **Photoproduction of Dijets with High Transverse Momenta at HERA**,
H1-Collaboration**, A. Aktas *et al.*, DESY 06 – 020, hep-ex/0603014, submitted to Phys.Lett. **B** (2006).
- [17] **Diffraction Photoproduction of ρ Mesons with High Transverse Momenta at HERA**,
H1-Collaboration**, A. Aktas *et al.*, DESY 06 – 023, hep-ex/0603038, submitted to Phys.Lett. **B** (2006).
- [18] **Search for Doubly-Charged Higgs Boson Production at HERA**,
H1-Collaboration**, A. Aktas *et al.*, DESY 06 – 038, hep-ex/0604027, submitted to Phys.Lett. **B** (2006).
- [19] Contributed papers by the H1-Collaboration to EPS2005/HEP2005: Int. Europhysics Conf. on High Energy Physics, Lisbon (Portugal), July 21-27, 2005 and to LEPTON-PHOTON 2005, XXII. Int. Symp. on Lepton-Photon Interactions at High-Energy, Uppsala, Sweden, June 30 - July 5, 2005. Only those papers are listed, which have not yet been submitted to journals.
- [20] **Measurement of the Polarisation Dependence of the Total e^-p Charged Current Cross Section** [19] (621,388)
- [21] **Multi-jet Production in High Q^2 Neutral Current Deep Inelastic Scattering at HERA and Determination of α_s** [19] (625,390)
- [22] **Inclusive Jet Production in Deep Inelastic Scattering at High Q^2 at HERA** [19] (629)
- [23] **Photoproduction of $D^{*\pm}$ Mesons Associated with a Jet at HERA** [19] (648,406)
- [24] **The Charm Fragmentation Function in DIS** [19](649,407)
- [25] **The Structure of Charm Jets in DIS** [19] (650,408)
- [26] **Study of Jet Shapes in Charm Photoproduction at HERA** [19] (651,409)
- [27] **Multi-lepton Events at HERA and a Generic Search for New Phenomena at Large Transverse Momentum** [19] (635,420); an updated analysis of the multilepton channel is available as report H1-prelim-06-063 (http://www-h1.desy.de/publications/H1preliminary.short_list.html)
- [28] **Events with an Isolated Lepton and Missing Transverse Momentum at HERA** [19] (637,421); an updated analysis is available as report H1-prelim-05-164_PRC_Nov05 (http://www-h1.desy.de/psfiles/confpap/EPS2005/H1-prelim-05-164_PRC_Nov05.ps)
- [29] **Acceptance Corrected Ratios of $D^*p(3100)$ and D^* Yields and Differential Cross Sections of $D^*p(3100)$ production** [19] (643,401)
- [30] **H1 Search for a Narrow Baryonic Resonance Decaying to $K_s^0p(\bar{p})$** [19] (644,400)
- [31] **Dijets in Photoproduction** [19] (680)

- [32] **First Measurement of Charged Current Cross Sections at HERA with Longitudinally Polarized Positrons**, H1-Collaboration**, A. Aktas et al., DESY 05 – 249, hep-ex/0512060, Phys.Lett.**B634** (2006), 173 - 179.
- [33] **Searches for Leptoquarks and for Lepton Flavor Violation with the H1-Experiment**, L. Lindfeld, Proc. 13. Int. Workshop on Deep Inelastic Scattering, Madison, Wisconsin, USA, April 27 - May 1, 2005, AIP. Conf. Proc. 792 (2005), 631 - 634.
- [34] **Search for Leptoquarks and Lepton Flavor Violation at HERA**, S. Schmitt, Proc. EPS Int. Europhysics Conf. on High Energy Physics, Lisbon, Portugal July 21 - 27, 2005, PoS HEPO2005 (2006), 316 - 319.
- [35] J. A. M. Vermaseren, Nucl. Phys. B **229** (1983) 347.
- [36] U. Baur, J. A. M. Vermaseren and D. Zeppenfeld, Nucl. Phys. B **375** (1992) 3.
- [37] T. Ahmed *et al.* [H1 Collaboration], DESY 94-248 (1994).
- [38] C. Adloff *et al.* [H1 Collaboration], Eur. Phys. J. C **5** (1998) 575 [hep-ex/9806009].
- [39] V. Andreev *et al.* [H1 Collaboration], Phys. Lett. B **561** (2003) 241 [hep-ex/0301030].
- [40] J.C. Pati and A. Salam, Phys. Rev. D **81** (1974) 275;
H. Georgi and S.L. Glashow, Phys. Rev. Lett. **32** (1974) 438;
P. Langacker, Phys. Rep. **72** (1981) 185.
- [41] H.P. Nilles, Phys. Rep. **110** (1984) 1;
H.E. Haber and G.L. Kane, Phys. Rep. **117** (1985) 75.
- [42] B. Schrempp and F. Schrempp, Phys. Lett. B **153** (1985) 101;
J. Wudka, Phys. Lett. B **167** (1986) 337.
- [43] S. Dimopoulos and L. Susskind, Nucl. Phys. B **155** (1979) 237; S. Dimopoulos, Nucl. Phys. B **168** (1980) 69; E. Farhi and L. Susskind, Phys. Rev. D **20** (1979) 3404; E. Farhi and L. Susskind, Phys. Rep. **74** (1981) 277.
- [44] W. Buchmüller, R. Rückl and D. Wyler, Phys. Lett. B **191** (1987) 442.
- [45] A. Aktas *et al.* [H1 Collaboration], Phys. Lett. B **629** (2005) 9 [hep-ex/0506044].
- [46] J. Breitweg *et al.* [ZEUS Collaboration], Phys. Lett.**B 472** (2000) 175 [hep-ex/9910045].
- [47] A. Aktas *et al.* [H1 Collaboration], Eur. Phys. J.**C38** (2005) 437 [hep-ex/0407018].
- [48] S. Chekanov *et al.* [ZEUS Collaboration], Phys. Lett.**B 595** (2004) 86 [hep-ex/0402019].
- [49] A. Gehrman-De Ridder, T. Gehrmann and E. Poulsen, Phys. Rev. Lett. **96** (2006) 132002 [hep-ph/0601073].
- [50] A. Gehrman-De Ridder, T. Gehrmann and E. Poulsen [hep-ph/0604030].
- [51] I. Abt *et al.* [H1 Collaboration] Nucl. Instr. and Meth. **A 386** (1997) 310, *ibid*, 348.
- [52] T. Nicholls *et al.* [H1 SPACAL Group], Nucl. Instrum. Meth. A **374** (1996) 149.
- [53] B. Andrieu *et al.* [H1 Calorimeter Group Collaboration], Nucl. Instrum. Meth. **A336** (1993) 460.
- [54] E. W. N. Glover and A. G. Morgan, Z. Phys. C **62** (1994) 311.
- [55] D. Buskalic *et al.* [ALEPH Collaboration], Z. Phys. C **69** (1996) 365.
- [56] T. Sjöstrand *et al.*, PYTHIA 6.2 Physics and Manual [hep-ph/0108264].
- [57] G. Corcella *et al.*, HERWIG 6.5 Release Note **135** (2001) 128 [hep-ph/0210213].
- [58] H. Jung, Comput. Phys. Commun. **86** (1995) 147
(see also <http://www.desy.de/jung/rapgap.html>).
- [59] Stephen D. Ellis, Davison E. Soper, Phys.Rev. **D48** (1993) 3160 [hep-ph/9305266].